Manufacturing Technologies and Applications
MATECA

An Investigation of Machinability of Hot Work Tool Steel Toolox 44 with Cutting Tools with Different Nose Radius Using Machine Learning

Kübra Kaya[1], Tayfun Çetin[2,*], Rüstem Binali[1], Hakan Gündoğmuş[3]

[1] Selçuk University, Department of Mechanical Engineering, 42075, Konya, Türkiye
[2] Hakkari University, Department of Electricity and Energy, Yüksekova Vocational School, 30000, Hakkari, Türkiye
[3] Hakkari University, Department of Mechanical Engineering, 30000, Hakkari, Türkiye

ABSTRACT

The advancement of technology has provided a new perspective for the manufacturing industry, accelerating research on machinability studies. The evaluation of key output parameters such as cutting force and temperature, surface roughness concerning input parameters (cutting speed, feed, depth of cut) is among the most common and comprehensive research topics in this field. In this study, dry turning operations were performed on Toolox 44 tool steel using input parameters of two varied feed rates (0.17, 0.34 mm/rev), two dissimilar cutting depths (0.2 mm, 0.4 mm), two distinct cutting speeds (40, 60 m/min), two different cutting tool nose radius (0.4 mm, 0.8 mm). The resulting parameters, including cutting temperature, force and surface roughness, were evaluated using graphical analysis and machine learning methods, specifically the decision tree and heat map approaches. The study's findings indicated that as the feed coupled with cutting depth enhanced, the cutting force also increased, whereas higher cutting speeds led to a decrease in the cutting force. Additionally, the reduction in cutting tool nose radius exhibited varying trends depending on different parameter combinations. It was determined that cutting temperature increased with higher feed and cutting depth, while the variation in cutting speed resulted in different increasing or decreasing trends in cutting temperature. The data revealed that surface roughness went up with an augment in feed, while it lowered as the cutting speed was raised. Additionally, an increase in cutting depth reduced surface roughness in the experiment set with a smaller tool nose radius, while it increased surface roughness in the experiment set with a larger tool nose radius. The results of the graphical evaluation were compared with those of another assessment method, namely machine learning, and it was found that there is a consistent level of accuracy between the two approaches. In the experimental setup with a 0.8 mm tool nose radius, cutting force, cutting temperature, and surface roughness increased by 187.73%, 20.05%, and 181.23%, respectively. For the 0.4 mm radius, the respective increases were 325.60%, 20.55%, and 132.52%. These results suggest that the 0.8 mm tool nose radius offers better machinability performance.

Keywords: *Toolox 44, Machinability, Different Radius, Tool Steel, Cutting Tools*

Farklı Burun Yarıçapına Sahip Kesici Takımlarla Toolox 44 Sıcak İş Takım Çeliğinin Makine Öğrenimi Kullanılarak İşlenebilirliğinin İncelenmesi

ÖZET

Teknolojinin ilerlemesi, imalat endüstrisi için yeni bir bakış açısı sağlayarak, işlenebilirlik çalışmaları üzerine yapılan araştırmaları hızlandırmıştır. Kesme kuvveti ve sıcaklığı, yüzey pürüzlülüğü gibi temel çıktı parametrelerinin girdi parametreleri (kesme hızı, ilerleme, kesme derinliği) açısından değerlendirilmesi bu alandaki en yaygın ve kapsamlı araştırma konularındandır. Bu çalışmada, Toolox 44 takım çeliği üzerinde iki farklı ilerleme hızı (0,17, 0,34 mm/dev), iki farklı kesme derinliği (0,2 mm, 0,4 mm), iki farklı kesme hızı (40, 60 m/dak), iki farklı kesici takım uç yarıçapı (0,4 mm, 0,8 mm) girdi parametreleri kullanılarak kuru tornalama işlemleri gerçekleştirilmiştir. Kesme sıcaklığı, kuvvet ve yüzey pürüzlülüğü dahil olmak üzere ortaya çıkan parametreler, grafiksel analiz ve makine öğrenmesi yöntemleri, özellikle karar ağacı ve ısı haritası yaklaşımları kullanılarak değerlendirilmiştir. Çalışmanın bulguları, kesme derinliğiyle birleştirilen ilerleme arttıkça kesme kuvvetinin de arttığını, buna karşın daha yüksek kesme hızlarının kesme kuvvetinde bir azalmaya yol açtığını göstermiştir. Ek olarak, kesici takım uç yarıçapındaki azalma farklı parametre kombinasyonlarına bağlı olarak farklı eğilimler sergiledi. Kesme sıcaklığının daha yüksek ilerleme ve kesme derinliği ile arttığı, kesme hızındaki değişimin ise kesme sıcaklığında farklı artan veya azalan eğilimlere yol açtığı belirlendi. Veriler, yüzey pürüzlülüğünün ilerlemedeki artışla arttığını, kesme hızı arttıkça ise azaldığını ortaya koydu. Ek olarak, kesme derinliğindeki artış, daha küçük takım uç yarıçapına sahip deney setinde yüzey pürüzlülüğünü azaltırken, daha büyük takım uç yarıçapına sahip deney setinde yüzey pürüzlülüğünü artırdı. Grafiksel değerlendirmenin sonuçları, başka bir değerlendirme yöntemi olan makine öğrenmesinin sonuçlarıyla karşılaştırıldı ve iki yaklaşım arasında tutarlı bir doğruluk düzeyi olduğu bulundu. 0,8 mm takım ucu yarıçaplı deneysel kurulumda, kesme kuvveti, kesme sıcaklığı ve

*Corresponding author, e-mail: tayfuncetin@hakkari.edu.tr

Received 21.02.2025; Revised 09.05.2025 Accepted 03.06.2025
https://doi.org/10.52795/mateca.1644170
To cite this article: K. Kaya, T. Çetin, R. Binali, H. Gündoğmuş, An Investigation of Machinability of Hot Work Tool Steel Toolox 44 with Cutting Tools with Different Nose Radius Using Machine Learning, Manufacturing Technologies and Applications 6(2) (2025) 164-183.

yüzey pürüzlülüğü sırasıyla %187,73, %20,05 ve %181,23 oranında arttı. 0,4 mm yarıçap için sırasıyla artışlar %325,60, %20,55 ve %132,52 oldu. Bu sonuçlar, 0,8 mm takım ucu yarıçapının daha iyi işlenebilirlik performansı sunduğunu göstermektedir.

Anahtar Kelimeler: *Toolox 44, İşlenebilirlik, Farklı Yarıçap, Takım Çeliği, Kesici Takımlar*

1. INTRODUCTION

In the manufacturing industry, machining methods have had a significant range of applications from past to present. Given the diverse range of applications, the research and development of machining methods must increase in accordance with technological advancements. Because, despite the discovery and implementation of new manufacturing techniques, it is an undeniable fact that the reliance on conventional machining processes cannot be eliminated. For this reason, research on topics such as the adoption of an environmentally friendly approach in machining methods, providing economic advantages, and achieving optimal machining results continues without interruption. Turning is a machining process where a cutting tool extracts material removed as chips from a workpiece that rotates during the operation [1-3]. In this machining method, there are several key challenges in achieving optimal results from all aspects and ensuring sustainable production. The first of these is the significantly excessive energy consumption during the cutting process [4, 5]. Another challenge is the concerns regarding the cooling/lubrication fluids used during the cutting process, as they pose potential risks both to the environment and to the health of the operator performing the operation [6-8]. These two fundamental issues highlight the necessity of making turning and other machining methods more sustainable. Sustainable manufacturing is considered a technological advancement that aims to reduce energy consumption, minimize waste produced after processing, limit the use of harmful substances, and decrease the emission of dangerous greenhouse gases into the atmosphere [9, 10].

The machinability of the material being processed is a crucial factor in achieving sustainable manufacturing. By considering the machinability of the material, the environmental, economic, and social impacts of the production can be easily altered, enabling the realization of sustainable manufacturing. The machinability of a material is generally characterized by three key factors: the power consumption related to cutting forces, the quality and integrity of the surface and tool wear, which are mainly affected by tool wear [11]. At the same time, the machinability of a material also refers to the ability to perform the machining process with minimal effort. Accordingly, a material with good machinability is defined as one that causes minimal tool wear during the process, results in low power consumption, and maintains surface integrity after the process [12, 13]. From a different viewpoint, fine-tuning the machining variables applied during the process is essential to achieving the best material machinability. The selection of cutting parameters is facilitated by factors such as understanding the physical and compositional characteristics of the material and knowing the areas in which the material will be used.

Toolox 44 is a material known for being ready for production after processes such as tempering, pre-hardening, and stress-relieving are applied, and it is also recognized as a tool steel [14, 15]. Although Toolox 44 has a high hardness, it is a material that is easy to machine [16]. Toolox 44, which has good machinability in terms of surface quality, is used in various mold types (injection, rubber, forming and cutting, metal injection) as well as in machine components [17]. Due to its low residual stress, Toolox 44 not only ensures dimensional accuracy easily during the machining process but is also characterized by its exceptional strength [14].

In the turning process, feed, cutting depth and speed can be given as examples of the applied cutting variables [18]. In addition to this, the primary factor altering the surface integrity and quality of the workpiece is the cutting tools. The compatibility of the cutting tool material with the workpiece material, together with factors such as the cutting tool configuration, also affect machinability and, consequently, help determine whether sustainable production can be realized. The following provides a summary of the studies in literature that investigate the influence of choosing processing parameters and tool geometry on output parameters.

Bayraktar et al. [19] assessed the machinability of Nimax and Toolox 44 tool steels during the milling process by varying depth, cutting speed, and keeping the feed constant, with a focus on analyzing cutting force and surface roughness. Following their research, optimum results for Toolox 44 were achieved with the use of low machining speed and feed parameters. Kuram et al. [20] performed a turning process on Toolox 44 steel and examined the impactof cutting speed, tool nose radius and feed on surface roughness. Due to their study, they found that as the tool nose radius expanded, the surface roughness values reduced for all cutting speeds considered. They reported that the most substantial parameter influencing surface roughness was feed, after tool nose radius and cutting speed in terms of their influence. Ribeiro et al. [21] carried out end milling on Toolox 44 steel using various cutting parameters to evaluate the surface quality after machining. They reported

that to achieve lower surface roughness values in a dry cutting environment, the axial depth of cut should be kept at lower levels. Furthermore, they observed that the surface roughness values in the dry cutting environment were smaller than those recorded in the other cutting environments. Panda et al. [22] studied the influence of cutting parameters, including cutting speed, depth, tool nose radius and feed, on the surface roughness in the process of hard turning of AISI 4340 steel. As a conclusion of their research, researchers reported that the tool nose radius and feed were the leading contributors for minimizing surface roughness. They also found that ceramic-coated tools provided an efficient alternative to CBN-coated and high-cost cutting tools. In his study, Akgün [23] investigated the parameters affecting cutting force, surface roughness, and power consumption during the turning of AISI 1040 steel. He concluded that feed rate is the most significant factor influencing all three output parameters. Mohanraj et al. [24] investigated the extent to which various output parameters are influenced by cutting parameters during the milling of Inconel 625. They concluded that surface roughness is affected by feed rate, tool flank wear is influenced by cutting speed, and machine vibrations are more significantly affected by cutting speed than by depth of cut. Rao et al. [25] investigated the effect of nose radius on cutting force and tool wear rate during dry turning of Inconel 718. They reported that cutting forces decreased with increasing cutting speed due to the rise in temperature and decreased with increasing tool nose radius. Tagiuri et al. [26] investigated the effect of the interaction between tool nose geometry and cutting parameters on machinability during the machining of AISI 1045 steel. The study revealed that these interactions significantly affect cutting stress, while their influence on tool wear and cutting temperature is relatively minor. Das et al. [27] assessed the machinability of AISI 4140 steel employing ceramic inserts with a PVD-TiN coating, combined with Al_2O_3 and TiCN in a hard turning operation. Within their research, conducted with various cutting parameters, surface roughness and flank wear were analyzed as output parameters. As a result, they reported that the key factor influencing surface roughness was feed, while flank wear was influenced by the interaction of all three parameters. Fang et al. [28] studied how tool wear impacts cutting force and vibrations during the high-speed finishing operation of the nickel-based superalloy Inconel 718. In their study, conducted by using cutting tools with different tool nose radius, they reported that an enhance in tool nose radius led to greater tool edge wear, resulting in an upward trend in cutting force values. Additionally, they noted that as tool edge wear increased, vibration also showed a corresponding increase. Shah et al. [29] evaluated the impact of several input factors, such as the feed rate, depth, cutting speed, and tool nose radius, on the resulting parameters like temperature during cutting, force applied, and the roughness of the surface during the turning process of Ti-6Al-4V material. It was determined that to achieve minimal cutting force, selecting a cutting speed of 315 rpm, a feed rate of 0.0510 mm/rev, a depth of 0.5 mm, and a tool nose radius of 0.4 mm would be optimal. In terms of surface roughness, the preferred parameters were a cutting speed of 140 rpm, a feed rate of 0.0510 mm/rev, a depth of 0.7 mm, and a tool nose radius of 1.2 mm. Lastly, to achieve the lowest cutting temperature, it was recommended to use a cutting speed of 140 rpm, a feed rate of 0.0510 mm/rev, a depth of cut of 1 mm, and a tool nose radius of 0.8 mm. In his study, Bhushan [30] studied how the tool nose radius and processing variables influence surface quality and tool life during the dry turning of AA7075/SiC composites. The study revealed that the minimum surface roughness value was achieved with a 1.2 mm tool nose radius, while maximum tool life was obtained with a 0.4 mm tool nose radius. He reported that the cutting depth and tool nose radius were the most considerable elements influencing surface roughness, and a larger tool nose radius led to lower surface roughness. Furthermore, it was observed that higher cutting speeds and feeds caused a decline in tool life. Saglam et al. [31] performed turning process to assess the role of rake angle and cutting speed in tool geometry on tool nose temperature and cutting force. Based on their findings, they found that the rake angle influenced the components of cutting force, whereas cutting speed influenced the tool nose temperature. Wang et al. [32] employed response surface methodology to evaluate how cutting parameters influence cutting temperature and cutting force during the milling of carbon fiber-reinforced polymer composites. The findings of the analysis revealed that the most crucial parameter affecting cutting temperature was spindle speed, whereas the feed was identified as the primary factor influencing cutting force. Akgün et al. [33] focused the impact of aging treatment on the material's machinability of T6 heat-treated AA7075 aluminum alloy by examining the influence of cutting tool nose radius and machining parameters on surface roughness. As a result, they achieved the optimum surface roughness for both the base material and the heat-treated material using a cutting tool nose radius of 1.2 mm, feed rate of 0.07 mm/rev, and cutting speed of 200 m/min. According to the analysis of variance, the most significant parameter affecting surface roughness for both materials was feed rate, and they also reported that an increase in tool nose radius led to a reduction in roughness. In another study, Akgün et al. [34] conducted research experiments on Mg alloy material reinforced with Mg_2Si after it was produced using the traditional casting method, followed by turning. The research assessed the impacts of cutting parameters (Four distinct cutting speeds and two feed), tool nose radius (two varying values) on surface roughness. The lowest surface

roughness was attained with a cutting speed of 350 m/min, a feed of 0.1 mm/rev, and a tool nose radius of 0.8 mm. It results showed that feed rate had the greatest influence on surface roughness, and an growth in tool nose radius was associated with a decline in surface roughness rates.

As seen in the literature review, there are numerous research examining the changes in output cutting parameters for various work materials using different manufacturing methods. To date, the combined effects of tool nose radius, feed rate, cutting speed, and depth of cut on Toolox 44 material have not been thoroughly investigated using both graphical analysis and machine learning techniques. Therefore, this study aims to provide a solid foundation for future research in this area.

2. MATERIAL AND METHOD

2.1. Experimental Setup

In this study, Toolox 44, which is widely recognized in literature as a tool steel material, was designated as the work material. The machining length of the workpiece is 200mm and the diameter is 50mm. The experiments were designed using a full factorial approach, and the machining parameters applied are shown in Table 1. Cutting parameters were determined according to the recommendations given by the cutting tool company. The chemical composition of Toolox 44 material is provided in Table 2. Table 3 presents the mechanical properties of the Toolox 44 material. The machinability of the workpiece was evaluated based on data obtained from 16 different experimental trials. Experiments were implemented under dry cutting conditions on a manual lathe. The cutting tools (carbide) used were CCMT-09T308-304 and CCMT-09T304-304, each with different tool nose radius. These cutting tools are produced by Korloy and have a TiC coating carbide. The experiments were conducted using a lathe manufactured by DE Lorenzo.

Table 1. The input machining parameters used in the experiments.

	Exp. Nu.	**Feed Rate (mm/rev)**	**Cutting Depth (mm)**	**Cutting Speed (m/min)**
Tool Nose Radius 0.8	1	0.17	0.2	40
	2	0.17	0.2	60
	3	0.17	0.4	40
	4	0.17	0.4	60
	5	0.34	0.2	40
	6	0.34	0.2	60
	7	0.34	0.4	40
	8	0.34	0.4	60
	Exp. Nu.	**Feed Rate (mm/rev)**	**Cutting Depth (mm)**	**Cutting Speed (m/min)**
Tool Nose Radius 0.4	1	0.17	0.2	40
	2	0.17	0.2	60
	3	0.17	0.4	40
	4	0.17	0.4	60
	5	0.34	0.2	40
	6	0.34	0.2	60
	7	0.34	0.4	40
	8	0.34	0.4	60

Table 2. Chemical composition of Toolox 44 tool steel [35].

Material	C	Si	Mn	S	P	Cr	Ni	Mo	V
Toolox 44	0.30	0.61	0.89	0.0009	0.010	1.23	0.66	0.79	0.145

Table 3. Mechanical properties of Toolox 44 tool steel [36].

Material	Hardness (HRC)	Yield strength $R_{p0.2}$ (MPa)	Tensile strength R_m (MPa)	Elongation, A5 (%)	Thermal conductivity (W/m·K)
Toolox 44	45	1300	1450	13	32

Cutting force was measured using a TeLC dynamometer integrated into the lathe, whereas cutting temperature was recorded by a TeLC sensor based on the radiation measurement method. The XKM2000 software program was used to record the cutting force and temperature during the experiments. The feed force was considered as the cutting force. The Mahr brand Perthometer M1 surface roughness measurement instrument was employed to quantify surface roughness, with 10 different measurements taken. The measurement length is 5.6 mm. Measurements were made at intervals of every 20 mm on the machined surface. The data obtained from the experiments were recorded using Excel and subjected to graphical analysis. Calibration of the devices used in the measurements was done using gauges specially produced for the devices. Roughness values were taken according to the average surface roughness (Ra) values occurring during machining on the workpiece according to ISO 4287. Additionally, the machine learning decision tree model, using the random forest method and a heatmap visualizing the correlation matrix showing the relationships between parameters, was created using the Python software program. Decision trees are divided into two categories according to the differences in the types of data processed: classification decision trees and regression decision trees. While classification decision trees are used when there is no relationship between the data, that is, when discrete data is considered and the result obtained by machine learning is a class belonging to the data, regression decision trees are used in continuous data and when a numerical value needs to be obtained in the predicted result. In other words, the purpose of using regression trees is to estimate the continuously dependent variable using continuous and categorical independent variables. The color of each square in the decision tree represents purity and the top node in the decision trees is called the root node. The root node is divided into branches and the branches into leaves, and this situation is likened to an inverted tree structure in the literature. Nodes whose result outputs are accepted as input by another node are called internal or test nodes, and those whose outputs are not presented as input to another node are called leaf nodes. In our study, the data was divided into 80% training and 20% testing, and the default parameters of the decision tree algorithm were used. Additionally, Pearson correlation analysis was performed for the heat map. Figure 1 presents a visual overview of the study conducted.

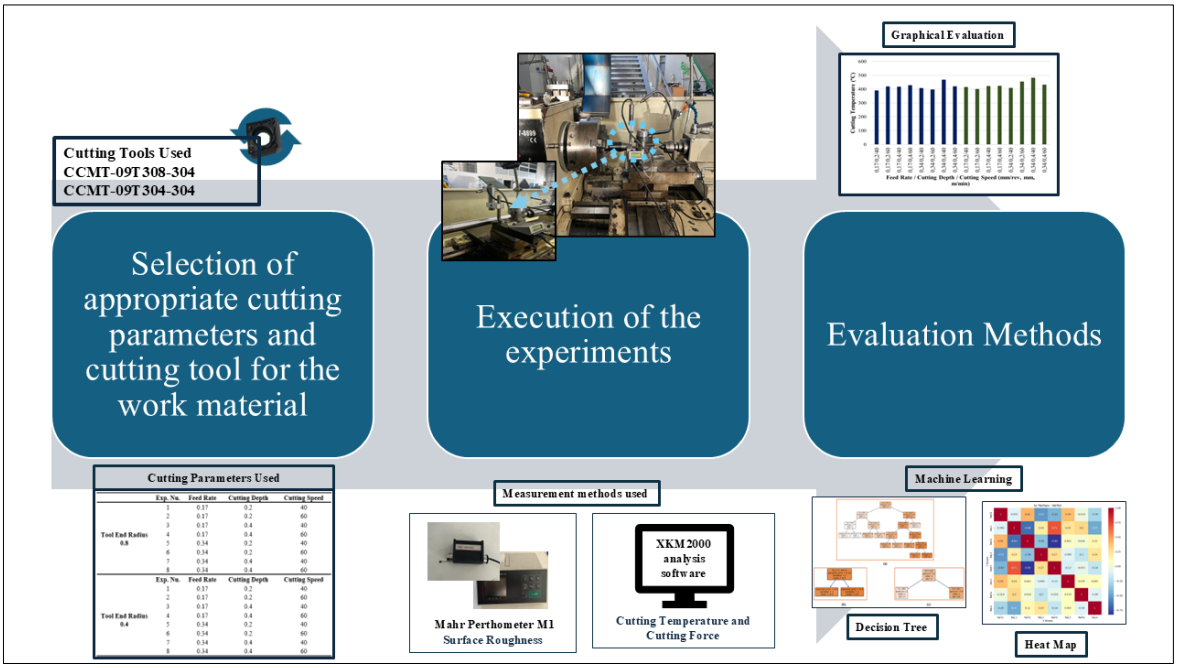

Figure 1. Graphical abstract of the realized study.

3. RESULTS AND DISCUSSION

In the study, the results gathered from the experiments will first be assessed graphically and secondly using machine learning methods, such as decision tree and heatmap techniques, to assess the response parameters including cutting force, temperature, and surface roughness. Each output parameter will be evaluated under different headings.

3.1 Cutting Force

Cutting force is recognized as a key parameter in determining machinability. The force that occurs in the cutting region, resulting from the contact between the cutting tool and the workpiece, is referred to as the cutting force [37-40]. Cutting speed, feed rate, cutting depth, primary and secondary cutting edge angles, tool nose radius, clearance angle, tool wear, and the physical and chemical characteristics of the workpiece material are factors that influence this output parameter [41].

Figure 2 provides the graphical evaluation of cutting force. Optimum cutting force values for both nose radius was obtained from the experiment conducted with the factors of 0.17 mm/rev feed, 0.2 mm cutting depth and 60 m/min cutting speed. The highest cutting force, conversely, was found for both the 0.8 mm and 0.4 mm end radii cutting tools in the experimental sets, with the parameters of 0.34 mm/rev feed, 0.4 mm depth of cut, and 60 m/min cutting speed. This suggests that higher feed values and the cutting depth parameters results in an expansion in force. Since both input parameters are related to the cutting area the rise in values results in higher friction which in turn escalations the cutting force [42]. In addition, as the feed rate increases, the chip thickness also increases, which in turn leads to higher cutting force values [43]. The increase in cutting force with increasing feed rate is consistent with findings reported in the literature [44-47]. Similarly, there are studies in the literature reporting that cutting forces increase with increasing cutting depth [48, 49]. For both nose radius, while maintaining constant feed and depth, an enhancement in cutting speed led to a reduction in cutting force. This situation may be attributed to the cutting tool contacting the workpiece for a shorter duration with the growth in cutting speed [50]. At the same time, as the cutting speed increases, more heat accumulates on the surface of the workpiece, leading to material softening. As a result, the workpiece becomes easier to machine, and the cutting forces tend to decrease [43, 51, 52]. In the experimental set with a 0.8 mm tool nose radius, a 187.73% increase in minimum and maximum cutting force values was observed, while in the 0.4 mm tool nose radius experimental set, this increase was calculated to be 325.60%. This leads to the conclusion that cutting tools with larger nose radius should be used for optimal cutting force values. In experiments with a 0.8 mm tool nose radius, a feed of 0.17 mm/rev, and a depth of cut of 0.2 mm, augmenting the cutting speed from 40 m/min to 60 m/min resulted in a 15.87% decrease in cutting force. In the trials where the cutting depth was maintained at 0.4 mm, a rise in cutting speed from 40 m/min to 60 m/min led to a decrease in cutting force by 35.40%. Higher cutting depths show that higher cutting speeds have a more significant positive effect on cutting force compared to lower cutting depths. Nonetheless, when the feed rate was raised to 0.34 mm/rev, the situation reversed, and it was found that using higher cutting speeds in cases of lower cutting depth had a greater positive impact on achieving the optimum cutting force. This result can be attributed to the combined effect of increased feed rate and higher cutting speed, which reduce the contact time between the tool and the workpiece, reducing the friction coefficient, thus minimizing the cutting force, especially when the depth of cut is low [53]. In the experiment set with a 0.4 mm tool nose radius and a feed of 0.17 mm/rev, the results were like those with the 0.8 mm nose radius. Nevertheless, when the feed was raised to 0.34 mm/rev, the highest reduction in cutting force occurred in the experimental pair with a cutting depth of 0.4 mm. Considering this, it is observed that using high speed and high depth with the 0.4 mm tool nose radius results in optimum outcomes.

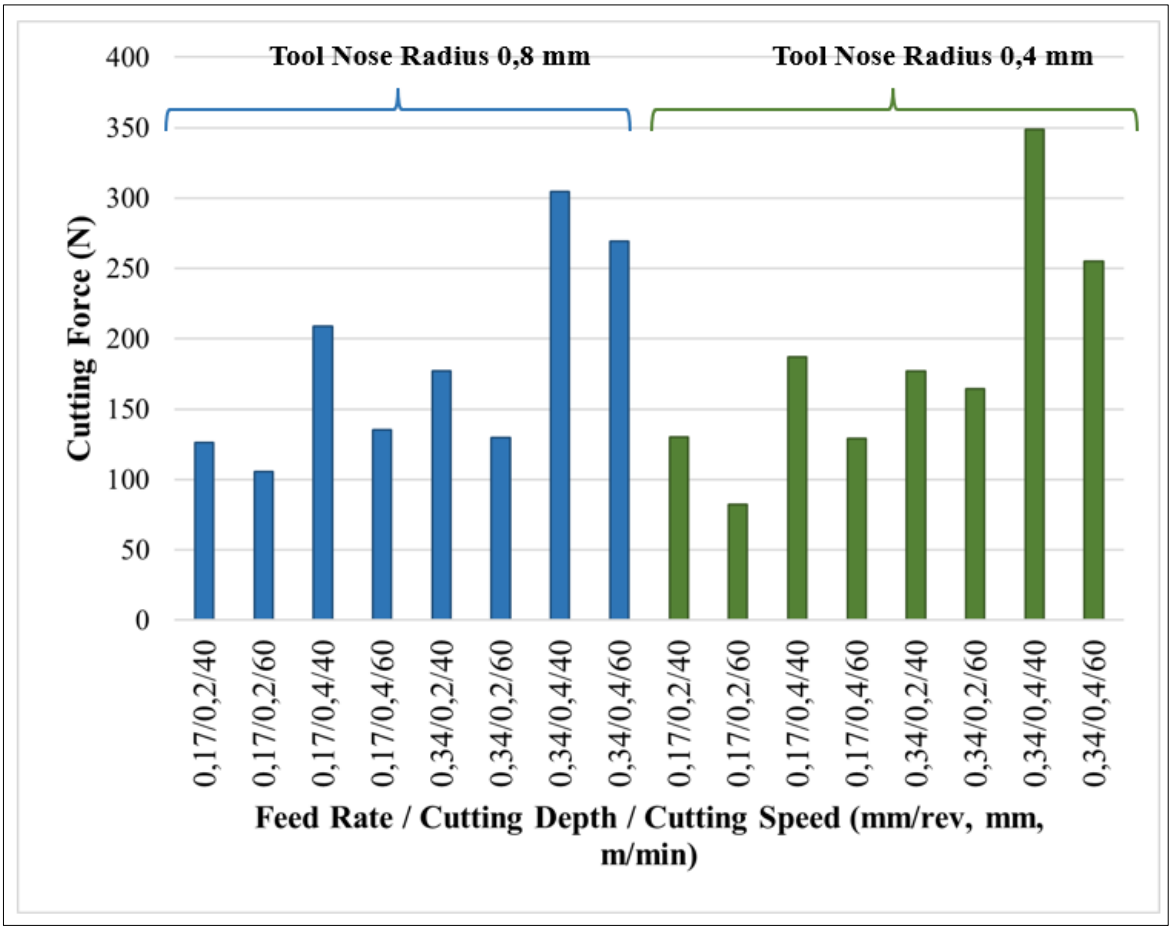

Figure 2. Graphical evaluation for cutting force parameter.

In Figure 3a, the decision tree for cutting force is presented. The squared error expression in decision trees is the square of the difference between the value predicted by the model and the actual value, and reflects how accurate the model estimate is. Samples is known as the number of samples in the data set that causes the branches in the decision tree, and value represents the average target value of the data group in the node. In other words, the interpretations made for the regression decision tree are made according to the numerical value shown by value. According to Figure 3a, the nodes with the highest cutting force have a value of 107. In Figure 3b, considering the branching of the decision tree, the experiment set with a cutting speed of 60 m/min, depth of 0.4 mm, and tool nose radius of 0.8 mm, with a feed of 0.17 mm/rev, corresponds to the left branch node with a value of 105. The experiment with a feed of 0.34 mm/rev belongs to the right branch node, with a value of 106.5. This suggests that an increase in feed rate leads to an escalation in force [54]. The reason for the increase in force is that as the feed rate increases, the volume of material removed per unit time and the contact area between the workpiece and the cutting tool increase, thus increasing the amount of power required for the cutting process [55, 56]. In Figure 3c, according to the decision tree section, for the experimental sets with a feed of 0.17 mm/rev, a speed of 60 m/min, and a tool nose radius of 0.8 mm, the experiment with a depth of 0.2 mm is represented by the left branch, which has a value of 104. When the cutting depth is set to 0.4 mm, it results in the right branch, which corresponds to a value of 106.286. This suggests that with an escalation in cutting depth, the cutting force values tend to rise. Like the rise in feed rate, the increase in cutting depth results in a larger cutting area between the cutting tool and the material [57]. Additionally, with the expansion of the cutting area, the cutting forces also tend to rise. With higher cutting speeds, the diminished contact time between the tool and the work material leads to a linear relationship with force, showing a decrease in cutting force [58]. A study in the literature reported that cutting forces tend to decrease with increasing cutting speed, as the resulting rise in cutting temperature facilitates easier machining of the material [59, 60]. This is why, in the decision tree model, the data from experiments conducted at a speed of 60 m/min were used, since the cutting forces noticed at this speed were reduced according to the experimental results. When the decision tree in Figure 3a is examined, the value at the node where the tool nose radius is 0.4 mm is 106.286. At the nodes where the tool nose radius is 0.8 mm, the values are read as 106.5 and 103.5, respectively. This suggests that the tool nose radius alone does not significantly affect the cutting force. Rather,

the selection of cutting parameters, whether high or low, leads to different results in cutting force. An advancement in tool nose radius can lead to higher cutting forces due to the wider contact region and higher resistance during cutting [25, 29]. However, at the same time, a larger nose radius can facilitate chip removal, reducing friction. Moreover, the ease of chip evacuation results in a decrease in temperature in the cutting zone, which lessens the negative effect of material adhesion on the force. As a result, the reduction in friction may cause a decline in cutting forces [61].

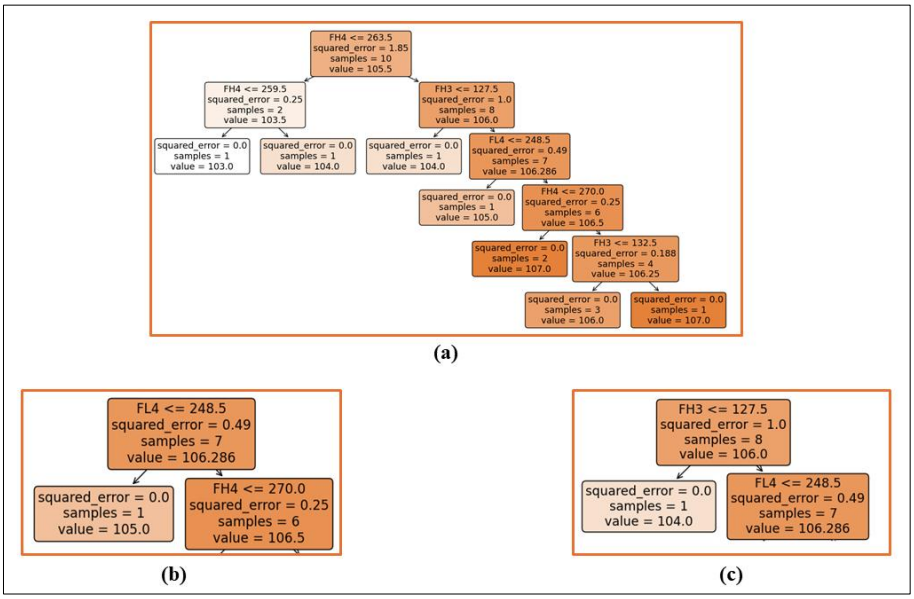

Figure 3. Decision tree model for cutting force.

Figure 4 displays the heatmap generated by visualizing the pearson correlation matrix for cutting force. In the figure, dark red squares represent positive correlations, while dark blue squares indicate negative correlations. In the figure, the letter 'H' denotes a nose radius of 0.8 mm, while 'L' represents a nose radius of 0.4 mm. Additionally, the numbers indicate the corresponding experiment numbers. The highest positive correlation is observed between the two experiments with tool nose radius of 0.4 and 0.8 mm. Despite the cutting parameters being the same in both experiments, the cutting force measured in the experiment with the 0.8 mm tool nose radius was higher compared to the experiment with the 0.4 mm tool nose radius. This indicates a positive correlation between the tool nose radius and cutting force, showing that as one increases, the other also increases. The growth of the tool nose radius consequences in a larger contact area within the interaction between the workpiece and the cutting zone, which in turn causes an elevation in cutting force [25]. Another positive correlation observed in the figure is found in the experimental set where the tool nose radius is 0.8 mm, the feed is 0.17 mm/rev, the cutting depth is increased from 0.2 to 0.4 mm, and the cutting speed is enhanced from 40 to 60 m/min. The rise in cutting force as the depth escalations shows a direct relationship across cutting depth and cutting force. Both parameters will show a trend of increasing and decreasing together [62-64]. The established positive correlation also point to that the increase in cutting speed could have an effect. However, by analyzing the figure, it can be inferred that the strongest negative correlation is observed between cutting speed and cutting force, indicating that a positive correlation exists between cutting depth and cutting force. In Figure 4, the highest negative correlation is observed in the experimental pair where the tool nose radius is 0.8 mm, the feed is 0.17 mm/rev, the depth of cut is 0.2 mm, and the cutting speed is increased from 40 m/min to 60 m/min. As cutting speed increases, cutting force decreases, demonstrating an inverse relationship [65, 66]. This situation can be attributed to the rises in temperature within the cutting area caused by the elevation of cutting speed, which facilitates chip removal and prevents chips from obstructing the cutting process on the workpiece [67]. As a result, cutting forces decrease.

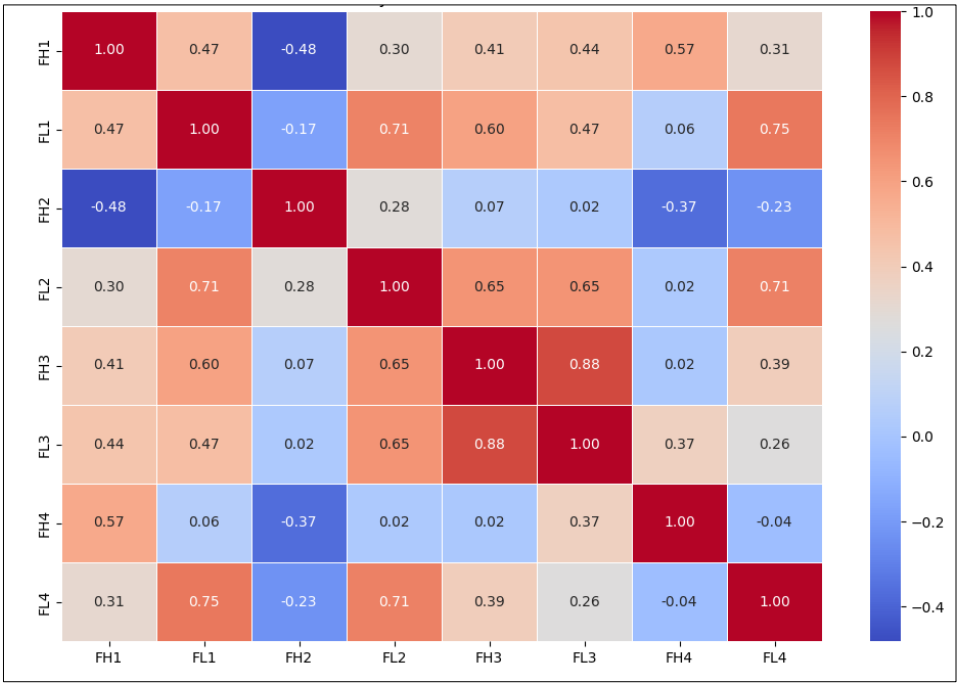

Figure 4. Heat map model for cutting force.

3.2. Cutting Temperature

The increased energy needed to extract a greater quantity of material in less time results in a rise in the heat produced near the cutting edge of the tool. In manufacturing, a substantial amount of the energy used is transformed into heat in the machining zone [68, 69]. The heat produced in the machining zone is dissipated through the tool, chips, workpiece, and coolant. Cutting temperature is crucial for tool life, surface finish, and the overall quality of the workpiece [70, 71]. Thus, it is crucial to examine how cutting parameters influence the changes in cutting temperature following the machining process.

Figure 5 shows the visual depiction of the cutting temperatures recorded after the experiments. In the experimental setup using a cutting tool with a 0.8 mm nose radius, the ideal cutting temperature was achieved at a cutting speed of 40 m/min, a feed of 0.17 mm/rev, and a depth of 0.2 mm. In the experimental configuration using a 0.4 mm cutting tool nose radius, the optimal cutting temperature was acquired at a cutting speed of 60 m/min, a feed of 0.17 mm/rev, and a depth of 0.2 mm. In the initial eight experiments (with a 0.8 mm cutting tool nose radius), a cutting speed elevation resulted in higher cutting temperatures in trials where the feed was 0.17 mm/rev and the depth was either 0.2 mm or 0.4 mm. However, when the feed was raised to 0.34 mm/rev, a rise in cutting speed led to lower cutting temperatures at both cutting depth levels. This indicates that the feed has a greater influence on cutting temperatures. When the feed rate rises, the volume of material extracted per unit time also increases, and the enhanced chip removal from the cutting zone contributes to lowering cutting temperatures [72]. The more chips are evacuated from the environment cutting each time, the more rapidly the cutting temperature tends to decrease [73]. In the experimental set with a cutting tool nose radius of 0.4 mm, a different trend in cutting temperature was seen in each experiment, with the feed and depth of cut kept constant. When the feed and cutting depths are low, increasing cutting speed results in a reduction of cutting temperature. However, at low feeds and higher cutting depths, a rise in cutting speed leads to an increase in cutting temperature [74-76]. Under conditions of high feed rates and shallow cutting depths, an increase in cutting speed raises the cutting temperature. Conversely, when both feed rate and cutting depth are high, an increase in cutting speed leads to a reduction in cutting temperature. In the experiment where the tool nose radius is 0.8 mm, the depth is 0.2 mm, and the cutting speed is 40 m/min, increasing the feed to 0.34 mm/rev leads to an increase in cutting temperature. In the experimental set with a 0.4 mm tool nose radius and identical parameters, raising the feed rate results in a reduction in cutting temperature.

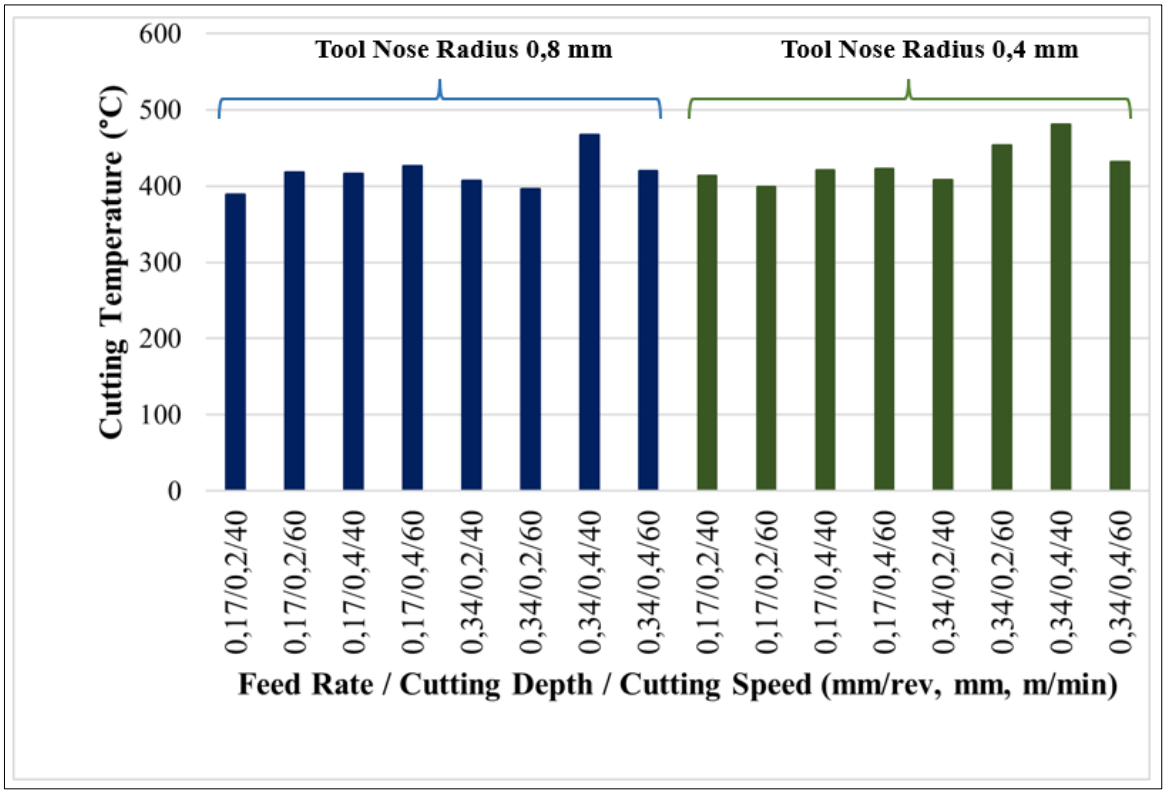

Figure 5. Graphical evaluation for cutting temperature parameters.

In Figure 6, the decision tree for cutting temperature is presented. In Figure 6a, the darkest colored nodes with the highest value predictions represent the nodes where the highest cutting temperature is expected. According to Figure 6a, the node with the value of 427.625 on the right side is the node where the highest cutting temperature is expected In the decision tree, the letter "T" represents cutting temperature, while "H" refers to cutting tool radius of 0.8 mm and "L" refers to cutting tool radius of 0.4 mm. According to this information, the highest value of 427.625 corresponds to a node with a cutting tool radius of 0.4 mm, whereas the value of 424.375 on the opposite branch corresponds to a node with a cutting tool radius of 0.8 mm. This suggests that a smaller cutting tool radius results in a rise in cutting temperature. In Figure 6b, for the experimental set using a cutting tool with a 0.4 mm radius, when the cutting speed is 60 m/min and the depth is 0.2 mm, experiments with higher feed rates lead to the right branch of the tree, resulting in a value of 420.5. Conversely, experiments with lower feed rates direct to the left branch, giving a value of 418.875. A similar situation is observed in the experiment set with a 0.8 mm cutting tool radius, where a cutting speed of 60 m/min and a depth of 0.4 mm are used, and the feed rate is raised from 0.17 mm/rev to 0.34 mm/rev. According to this, increasing the feed rate leads to higher chip removal rates, which in turn increases cutting forces, power consumption, and friction [77, 78]. With a rises in cutting force, there is also a rise in cutting temperature within the cutting zone. In Figure 6c, for the experimental set with a 0.8 mm cutting tool radius, a cutting speed of 40 m/min, a feed of 0.34 mm/rev, and a depth of 0.2 mm are associated with the left branch of the decision tree, while a depth of 0.4 mm is associated with the right branch. The corresponding value results are 423.75 and 425, respectively. This indicates that, like the effect of an increase in feed rate, a rise in cutting depth also results in higher cutting temperatures [79]. With an increased cutting depth, the interaction zone between the cutting tool and the workpiece expands [80]. This increase in contact area causes higher friction and consequently, cutting forces and power consumption also rise, which causes the cutting temperature to increase as well.

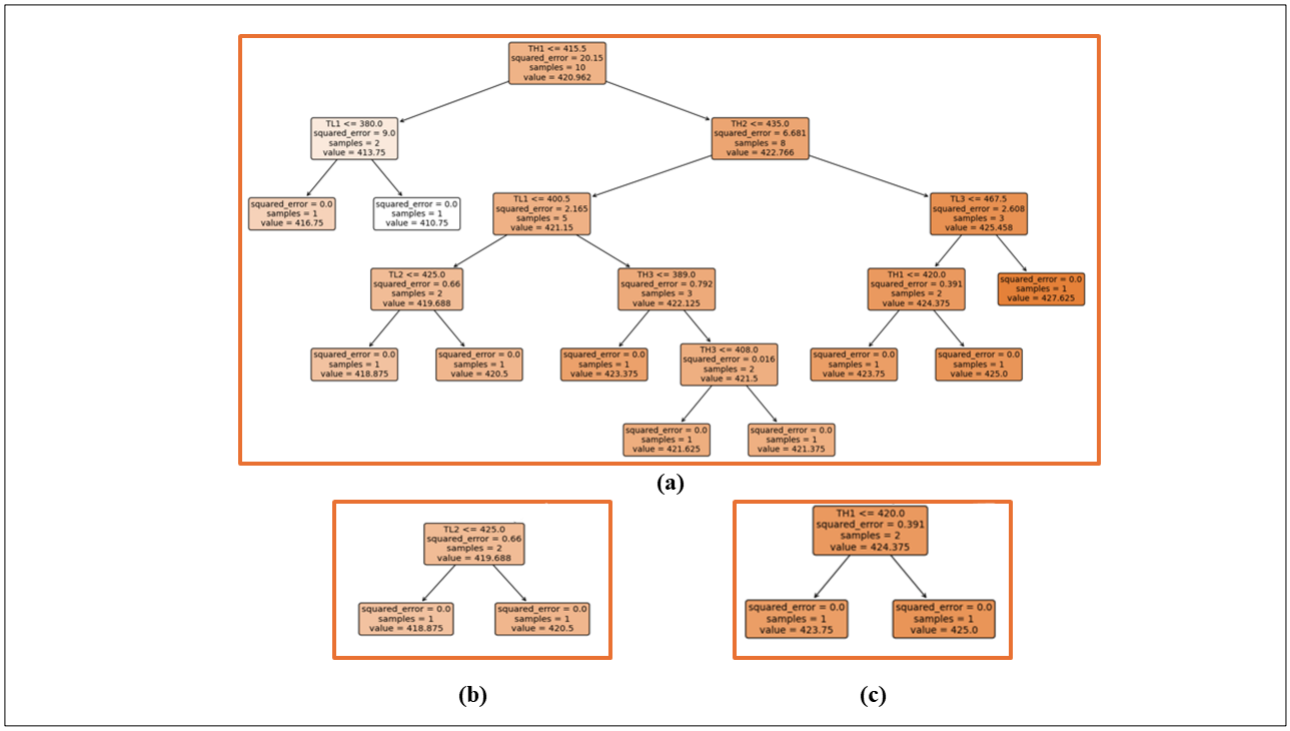

Figure 6. Decision tree model for cutting temperature.

In Figure 7, the heat map for cutting temperature is presented. The dark red colors represent positive correlation, while the dark green colors represent negative correlation. The darkest green colors, representing the relationship between each parameter and itself, are located along the diagonal of the heat map. The strongest positive relationship between TL1 and TL4 appears in the experimental group featuring a 0.4 mm cutting tool radius, particularly in Experiments 1 and 4. In these experiments, with the feed maintained at 0.17 mm/rev, the cutting depth is raised from 0.2 mm to 0.4 mm, and the cutting speed is increased from 40 m/min to 60 m/min. Simultaneously, the cutting temperature increases in parallel. This implies that cutting depth and cutting speed are positively correlated, with an increase in either of these parameters leading to an augment in cutting temperature. As the depth becomes greater, the interaction area between the cutting tool and the material expands, causing an increase in friction, which subsequently raises the cutting temperature [81]. Although the literature suggests that cutting temperatures decrease when cutting speed increases because of the decreased interaction time between the tool and the material, in some cases, the additional heat produced by the material's enhanced plastic deformation can cause a rise in cutting temperatures as the cutting speed increases [82]. Additionally, the fast and brief cutting operations can obstruct the proper expulsion of chips from the cutting area, resulting in an increase in the heat accumulation within the cutting zone [83]. When examining the positive correlation observed between TH4 and TL4, it becomes evident that the parameter changing in this experimental set is the cutting tool radius. This implies that changes in cutting tool radius can notably influence the cutting temperature, especially when other parameters, like cutting speed and feed rate, remain unchanged. As the cutting tool radius increases, it can result in a larger interaction surface between the tool and the material being machined, potentially enhancing friction and thus raising the cutting temperature. As the cutting tool radius is reduced, a corresponding decrease in the observed cutting temperature is noted. A reduced tool radius leads to lower friction, thereby decreasing the cutting forces. The reduction in cutting forces causes a decrease in cutting temperature [84]. Additionally, a smaller tool radius allows chips to be evacuated more easily from the cutting zone, which helps in reducing accumulated heat. In the heat map shown in Figure 7, the highest negative correlation is observed between TL2 and TH4, followed by a negative correlation between TL1 and TL2. The negative correlation observed between TL2 and TL4 indicates that as the tool radius and cutting depth decrease, the cutting temperature also decreases. However, the negative relationship found in the correlation matrix suggests that instead of a direct interaction between variables, indirect factors may be influencing the results. The distribution of the dataset or measurement deviations could be affecting this outcome, leading to the observed negative correlation between the variables. In general, a positive correlation between cutting speed and temperature is expected, but the observed negative correlation between TL1 and TL2 may be attributed to measurement errors, uncontrolled factors (such as the small tool

radius), or variations in experimental conditions. Furthermore, the combination of other parameters that lower cutting temperature, along with a rise in cutting speed, may explain this inverse relationship.

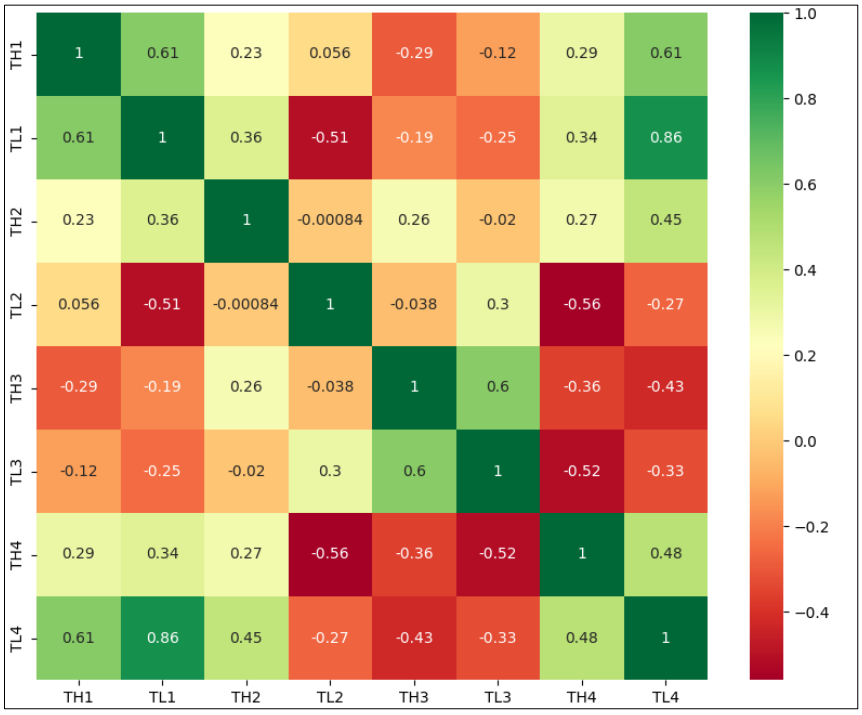

Figure 7. Heat map model for cutting temperature.

3.3. Surface Roughness

During the machining of the work material, on top of that to chemical and physical factors, variations in surface height occur due to the mechanical movements of the cutting tool on the workpiece surface. These deviations are referred to as surface roughness [85]. surface roughness is affected not only by factors that can be controlled but also by those that cannot be controlled [86]. Factors that impact surface roughness and can be managed by the operator during the machining process encompass cutting speed, depth, feed and the design of the cutting tool. Because surface roughness plays a crucial role in determining the quality and condition of the workpiece surface, it is significant to analyze this parameter [87].

Figure 8 presents a graphical evaluation of surface roughness measurements. In the experimental setup where the tool radius was 0.8 mm, the best surface finish was achieved using a feed of 0.17 mm/rev, a depth of 0.2 mm, and a cutting speed of 60 m/min. In the experiment set with a nose radius of 0.4 mm, the optimum surface roughness was acquired with the parameters of 0.17 mm/rev feed, 0.4 mm depth, and 60 m/min cutting speed. Based on this, it can be inferred that to achieve the best surface finish, increasing the depth is recommended when the tool radius is small. In the experiment set with a cutter radius of 0.8 mm, the highest roughness values were recorded with a feed of 0.34 mm/rev, a cutting depth of 0.4 mm, and a speed of 60 m/min. When the results are examined, the roughness values decrease with the increase in the nose radius. This increase leads to higher cutting temperatures due to greater friction between the tool and the surface. As a result, the chip is removed more easily, and a smoother surface is obtained [88]. For the experiment with a 0.4 mm cutter radius, the maximum roughness values were obtained with a feed rate of 0.34 mm/rev, a cutting depth of 0.2 mm, and a cutting speed of 40 m/min. In both cases, when the feed and depth were held constant, a rise in speed led to a reduction in surface roughness measurements [89]. The improvement in surface quality and the reduction in roughness values with increasing feed rate can be attributed to the rise in cutting temperature caused by higher cutting speeds, which facilitates material deformation and consequently leads to lower surface roughness [89]. Conversely, when the feed was raised (with constant cutter radius and cutting depth), the surface roughness also increased [90]. In the experiment set with a 0.8 mm cutter radius, surface roughness values increased as cutting depth increased, while keeping feed rate and cutting speed constant. On the other hand, in the experiment set with a 0.4 mm cutter radius, an increase in cutting depth, while keeping feed rate and cutting speed constant, led to a decrease in surface roughness values. In general, looking at Figure 8, high feed resulted in greater surface roughness values [91, 92]. High feed cause the cutting tool to remove more material with each revolution, leading to larger chip protrusions and fluctuations on the workpiece

surface, which reduces surface quality. At higher feed rates, the cutting tool exerts more pressure on the material, which increases tool vibrations and creates residual stresses due to increased heat generated between the tool and the workpiece surface. As a result, this contributes to a rougher surface [88, 93, 94].

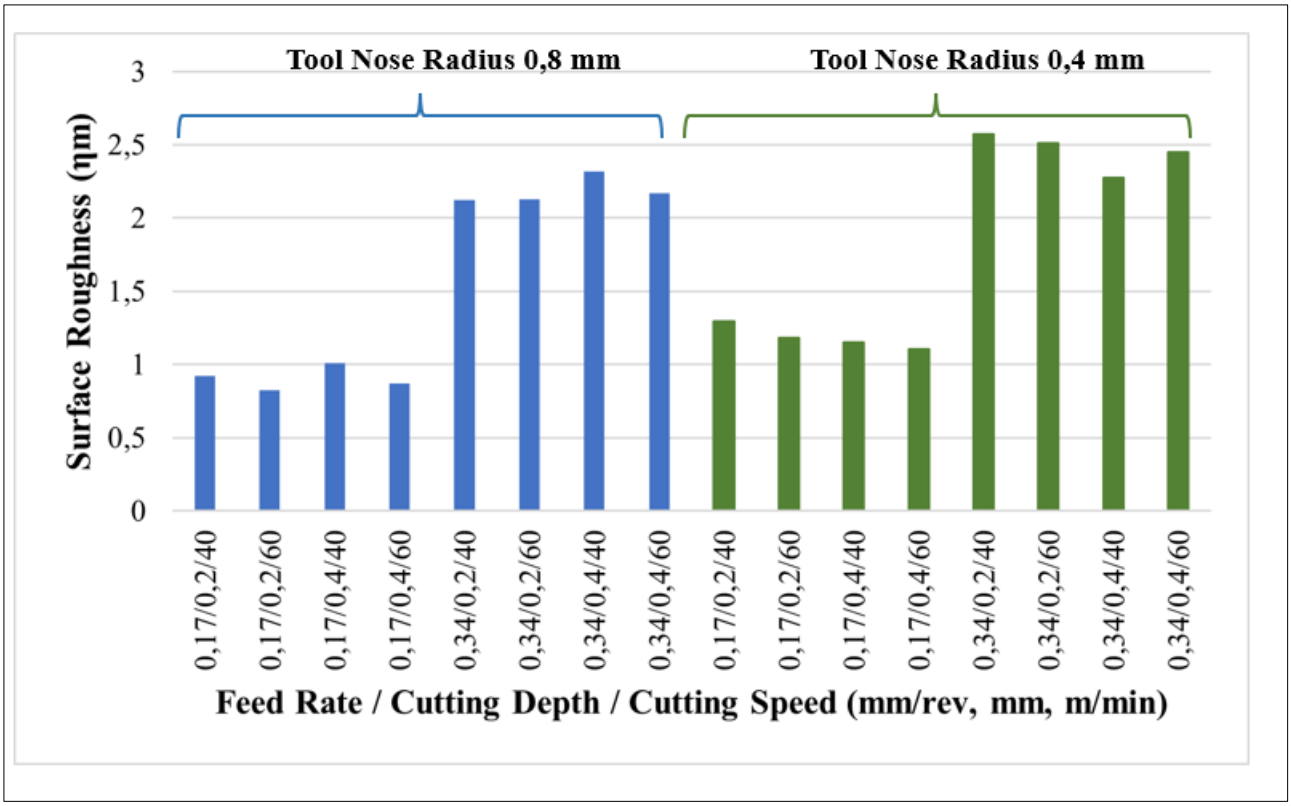

Figure 8. Graphical evaluation for surface roughness parameters.

Figure 9 displays a graphical depiction of the surface roughness data. In the decision tree shown in Figure 9a, the node with a value of 9 and the darkest color tone represents the point where the highest surface roughness values will be obtained. When the decision tree (Figure 9a) is examined, the letter "H" next to Ra indicates a cutting tool radius of 0.8 mm, while the letter "L" corresponds to a 0.4 mm cutting tool radius. From the data, it can be observed that an rises in the cutting tool radius is associated with higher surface roughness quantities. As the cutting tool radius increases, the tendency for plastic deformation and side flow during cutting increases, causing irregularities on the Surface [95]. Additionally, a larger tool radius makes chip formation more difficult, preventing the creation of a smooth surface and leading to higher surface roughness values. In Figure 9b, in the experiment set with a cutting tool radius of 0.4 mm, speed of 60 m/min, and depth of 0.4 mm, the 0.17 mm/rev feed corresponds to the node on the left with a value of 6.5, while the 0.34 mm/rev feed corresponds to the node on the right with a value of 8.5. This shows that increasing the feed results in higher surface roughness [96]. When the feed is elevated, the cutting tool moves more frequently within a given time frame, and the wavelength created by the tool tip expands, leaving more prominent marks on the surface. These surface irregularities increase, leading to a rise in surface roughness. In Figure 9c, in the experiment set with a cutting tool radius of 0.4 mm, feed of 0.17 mm/rev, and cutting speed of 60 m/min, the cutting depth of 0.2 mm corresponds to a node with a value of 1, while the experiment executed with a depth of 0.4 mm corresponds to a node with a value of 0. Here, a different result is obtained compared to the general trend, leading to the conclusion that as the cutting depth decreases, surface roughness values increase. As cutting depth decreases, the cutting tool removes smaller chips from the workpiece, which can cause irregularities in cutting forces and vibrations of the tool, thereby increasing surface roughness [97]. Additionally, at lower cutting depths, the duration of connection between the tool and the material shortens, and the cutting operation becomes less stable, resulting in the formation of irregularities on the surface.

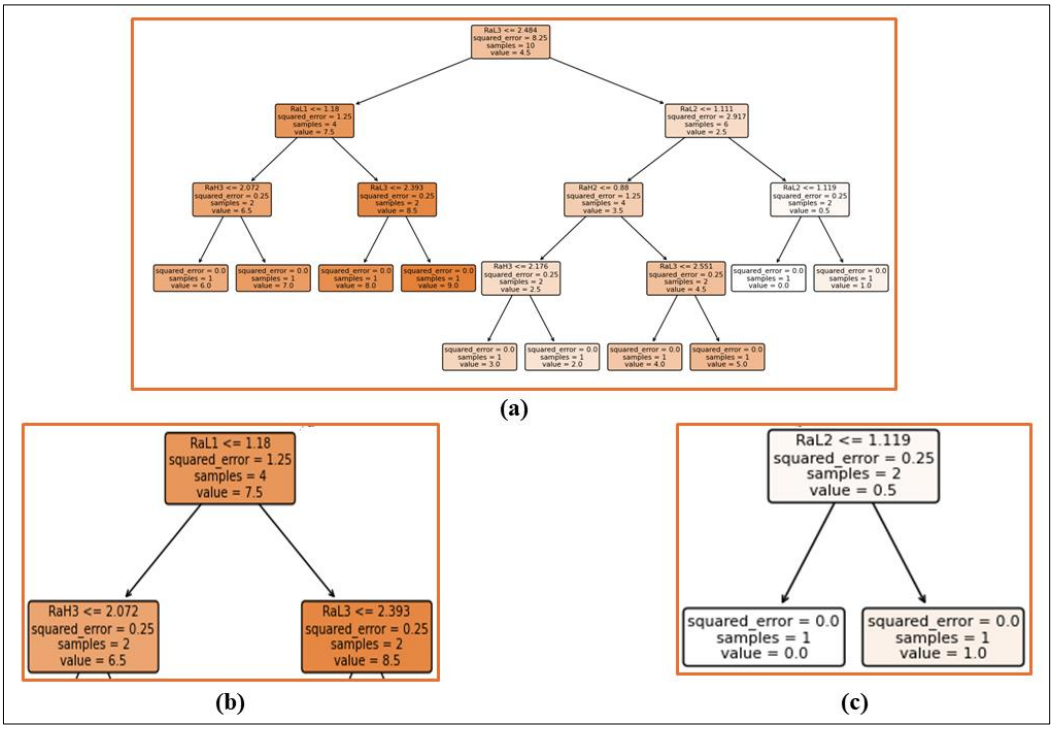

Figure 9. Decision tree model for surface roughness.

Figure 10 presents a heatmap of the correlation matrix created using surface roughness values. In the heatmap, dark red tones indicate positive correlations, while dark blue tones represent negative correlations. The highest positive correlation occurred between the parameters of the RaL1 and RaH3 experiments. In this experiment set, despite a reduction with respect to both the tool radius and depth, surface roughness increased. The observed positive correlation, even though cutting depth decreased while surface roughness increased, may be due to indirect interactions such as the simultaneous reduction of cutting depth and tool radius [98]. However, since the correlation shows the general trend of the variables rather than a direct cause-and-effect relationship, the distribution of the data set and measurement ranges may have generated a positive correlation despite this inverse relationship. This situation is attributed to the fact that the variables show a tendency to alteration together, but their effects can occur in different directions. In Figure 10, the highest negative correlation is observed between RaH2 and RaH3. In this experiment pair, the cutting tool radius is 0.8 mm, and the feed rate is fixed at 0.17 mm/rev. As the cutting depth rises from 0.2 to 0.4 mm, the cutting speed reduces from 60 to 40 m/min. In response to the change in parameters, surface roughness increased. Here, the inverse connection between cutting speed and surface finish resulted in the establishment of a negative correlation. At lower cutting speeds, the cutting tool creates more deformation on the material and increases the effect of plastic flow, leading to surface irregularities [99]. Additionally, at lower speeds, the cutting process progresses with a less sharp chip removal process, causing improper chip separation, which negatively affects surface quality and leads to an increase in roughness [100].

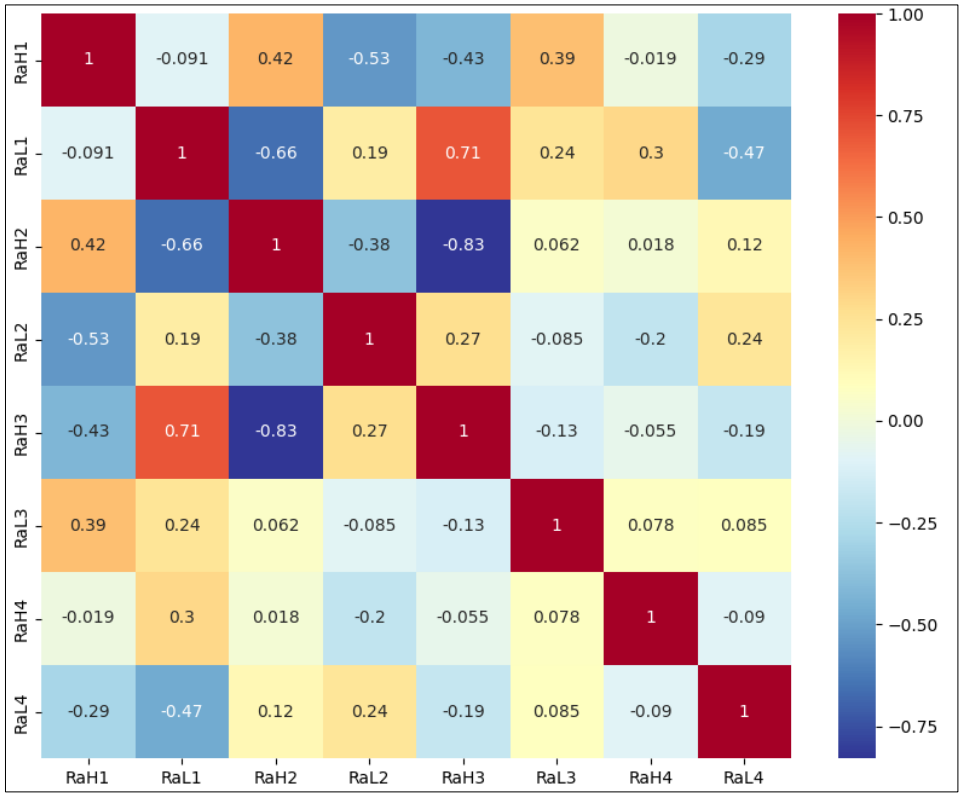

Figure 10. Heat map model for surface roughness.

4. CONCLUSIONS

In this research, dry turning tests were undertaken to examine how changes in feed rate, cutting depth, cutting speed, and tool radius affect key output parameters in machining, including cutting force, cutting temperature, and surface roughness. The findings of the study are summarized as follows:

- It was observed that cutting force rises as feed and cutting depth increase, while it declines when cutting speed is reduced. In the heat map generated for cutting force, the strongest positive relationship was seen between the cutting tool radius and cutting force, while the most significant negative correlation was identified between cutting speed and force. The optimum result for cutting force was found in the experiment with 0.4 nose radius tool, 0.17 mm/rev feed rate, 0.2 mm depth of cut and 60 m/min cutting speed.
- The escalation in cutting temperature occurred with the rises in feed and cutting depth, while the increase in cutting speed showed different trends of either decrease or increase in cutting temperature. Generally, cutting temperatures lowered with the increase in tool radius, although some cutting parameter combinations led to an increase. In the heat map created for cutting temperature, the highest positive correlation was established between cutting depth, cutting speed, and temperature. The optimum result for cutting temperature was found in the experiment with 0.8 nose radius tool, 0.17 mm/rev feed rate, 0.2 mm depth of cut and 40 m/min cutting speed.
- Surface roughness values escalated with the rise in feed, decreased with the increase in cutting speed, and the rises in cutting depth reduced surface roughness in the low tool radius experiment sets, while it increased surface roughness in the high tool radius sets. According to the surface roughness heat map, the highest positive correlation was observed between tool radius, cutting depth, and surface roughness. The highest negative correlation was found between cutting speed and surface roughness. The optimum result for surface roughness was found in the experiment with 0.8 nose radius tool, 0.17 mm/rev feed rate, 0.2 mm depth of cut and 40 m/min cutting speed.

ACKNOWLEDGMENT

This research was supported by Hakkari University, Scientific Research Project Coordination Unit (BAP; Grant no. FM24BAP8).

REFERENCES

[1] T. T. Le, H. T. Pham, H. Khac Doan, P. G. Asteris, Experimental and computational investigation of the effect of machining parameters on the turning process of C45 steel, Advances in Mechanical Engineering 17(2) (2025). https://doi.org/10.1177/16878132251318170.

[2] R. Binali, M. E. Korkmaz, M. T. Özdemir, M. Günay, A Holistic Perspective on Sustainable Machining of Al6082: Synergistic Effects of Nano-Enhanced Bio-Lubricants, Machines 13(4) (2025) 293. https://doi.org/10.3390/machines13040293.

[3] A. Ç. Yalçın, F. Şen, B. Divleli, T. Küçükçolak, C. Menşan, R. Binali, Finish turning of AISI 5140 tempered steel to improve machinability for engineering applications: An experimental approach with dry cutting, Doğu Fen Bilimleri Dergisi 6(2) (2024) 1-10. https://doi.org/10.57244/dfbd.1392858.

[4] K. Fang, N. Uhan, F. Zhao, J. W. Sutherland, A new approach to scheduling in manufacturing for power consumption and carbon footprint reduction, Journal of Manufacturing Systems 30(4) (2011) 234-240. https://doi.org/10.1016/j.jmsy.2011.08.004.

[5] M. K. Gupta, P. Niesłony, M. E. Korkmaz, M. Kuntoğlu, G. M. Królczyk, M. Günay, M. Sarikaya, Comparison of tool wear, surface morphology, specific cutting energy and cutting temperature in machining of titanium alloys under hybrid and green cooling strategies, International Journal of Precision Engineering and Manufacturing-Green Technology, 10(6) (2023) 1393-1406. https://doi.org/10.1007/s40684-023-00512-9.

[6] N. Bhanot, P. V. Rao, S. G. Deshmukh, An assessment of sustainability for turning process in an automobile firm, Procedia CIRP, 48 (2016) 538-543. https://doi.org/10.1016/j.procir.2016.03.024.

[7] M. Günay, M. E. Korkmaz, N. Yaşar, Performance analysis of coated carbide tool in turning of Nimonic 80A superalloy under different cutting environments, Journal of Manufacturing Processes, 56 (2020) 678-687. https://doi.org/10.1016/j.jmapro.2020.05.031.

[8] M. A. Makhesana, K. M. Patel, N. D. Ghetiya, R. Binali, M. Kuntoğlu, Evaluation of drilling and hole quality characteristics in green machining aluminium alloys: A new approach towards green machining, Journal of Manufacturing Processes, 129 (2024) 176-186. https://doi.org/10.1016/j.jmapro.2024.08.059.

[9] C. N. Madu, Handbook of environmentally conscious manufacturing, Springer Cham, 2001. https://doi.org/10.1007/978-3-030-75834-9.

[10] R. Binali, A. D. Patange, M. Kuntoğlu, T. Mikolajczyk, E. Salur, Energy saving by parametric optimization and advanced lubri-cooling techniques in the machining of composites and superalloys: A systematic review, Energies, 15(21) (2022) 8313. https://doi.org/10.3390/en15218313.

[11] Y. Isik, Investigating the machinability of tool steels in turning operations, Materials & design, 28(5) (2007) 1417-1424. https://doi.org/10.1016/j.matdes.2006.03.025.

[12] L. Dan, J. Mathew, Tool wear and failure monitoring techniques for turning—a review, International Journal of Machine Tools and Manufacture, 30(4) (1990) 579-598. https://doi.org/10.1016/0890-6955(90)90009-8.

[13] R. Binali, Experimental and machine learning comparison for measurement the machinability of nickel based alloy in pursuit of sustainability, Measurement, 236 (2024) 115-142. https://doi.org/10.1016/j.measurement.2024.115142.

[14] S. Globisch, M. Friedrich, N. Heidemann, F. Döpper, Tool concept for a solid carbide end mill for roughing and finishing of the tool steel Toolox 44, Journal of Manufacturing and Materials Processing, 8(4) (2024) 170. https://doi.org/10.3390/jmmp8040170.

[15] S. Naimi, S. M. Hosseini, Tool steels in die-casting utilization and increased mold life, Advances in Mechanical Engineering, 7(1) (2015) 286071. https://doi.org/10.1155/2014/286071.

[16] A. M. A. Al-Ahmari, Predictive machinability models for a selected hard material in turning operations, Journal of materials processing technology, 190(1-3) 2007 305-311. https://doi.org/10.1016/j.jmatprotec.2007.02.031.

[17] R. Binali, H. Demir, İ. Çiftçi, An Investigation into the Machinability of Hot Work Tool Steel (Toolox 44), 3rd Iron and Steel Symposium(UDCS'17), Karabuk-Turkey, 2017: 441-444.

[18] S. M. Darwish, The impact of the tool material and the cutting parameters on surface roughness of supermet 718 nickel superalloy, Journal of Materials Processing Technology, 97(1-3) (2000) 10-18. https://doi.org/10.1016/S0924-0136(99)00365-9.

[19] Ş. Bayraktar, G. Uzun, Ön sertleştirilmiş Toolox 44 ve Nimax kalıp çeliklerinin işlenebilirliği üzerine deneysel çalışma, Gazi Üniversitesi Mühendislik Mimarlık Fakültesi Dergisi, 36(4) (2021) 1939-1948. https://doi.org/10.17341/gazimmfd.641824.

[20] E. Kuram, N. Ucuncu, Toolox 44 Çeliğinin Tornalanmasında Kesme Hızının, İlerlemenin ve Kesici Uç Burun Radyüsünün Takım Aşınmasına ve Yüzey Pürüzlülüğüne Etkileri, Gazi Üniversitesi Fen Bilimleri Dergisi Part C: Tasarım ve Teknoloji, 12(4) (2024) 1006-1017. https://doi.org/10.29109/gujsc.1530456.

[21] M. B. A. Ribeiro, A. J. Souza, H. J. Amorim, Cobem2021-0118 Investigation Of Surface Roughness Generated By End Milling Of Toolox 44®, 26th ABCM International Congress of Mechanical Engineering, Florianópolis, SC, Brazil, 2021: 22-26.

[22] A. Panda, S. R. Das, D. Dhupal, Surface roughness analysis for economical feasibility study of coated ceramic tool in hard turning operation, Process Integration and Optimization for Sustainability, 1 (2017) 237-249. https://doi.org/10.1007/s41660-017-0019-9.

[23] M. Akgün, Optimization of process parameters affecting cutting force, power consumption and surface roughness using taguchi-based gray relational analysis in turning AISI 1040 steel, Surface Review and Letters, 29(03) (2022) 2250029. https://doi.org/10.1142/S0218625X22500299.
[24] T. Mohanraj, P. Ragav, E. S. Gokul, P. Senthil, K. S. R. Anandh, Experimental investigation of coconut oil with nanoboric acid during milling of Inconel 625 using Taguchi-Grey relational analysis, Surface Review and Letters, 28(03) (2021) 2150008. https://doi.org/10.1142/S0218625X21500086.
[25] A. S. Rao, Effect of nose radius on the chip morphology, cutting force and tool wear during dry turning of Inconel 718, Tribology-Materials, Surfaces & Interfaces, 17(1) (2023) 62-71. https://doi.org/10.1080/17515831.2022.2160161.
[26] Z. A. M. Tagiuri, T. M. Dao, A. M. Samuel, V. Songmene, A numerical model for predicting the effect of tool nose radius on machining process performance during orthogonal cutting of AISI 1045 steel, Materials, 15(9) (2022) 3369. https://doi.org/10.3390/ma15093369.
[27] S. R. Das, D. Dhupal, A. Kumar, Study of surface roughness and flank wear in hard turning of AISI 4140 steel with coated ceramic inserts, Journal of Mechanical Science and Technology, 29 (2015) 4329-4340. https://doi.org/10.1007/s12206-015-0931-2.
[28] N. Fang, P. S. Pai, S. Mosquea, Effect of tool edge wear on the cutting forces and vibrations in high-speed finish machining of Inconel 718: an experimental study and wavelet transform analysis, The International Journal of Advanced Manufacturing Technology, 52 (2011) 65-77. https://doi.org/10.1007/s00170-010-2703-6.
[29] D. Shah, S. Bhavsar, Effect of tool nose radius and machining parameters on cutting force, cutting temperature and surface roughness–an experimental study of Ti-6Al-4V (ELI), Materials Today: Proceedings, 22 (2020) 1977-1986. https://doi.org/10.1016/j.matpr.2020.03.163.
[30] R. K. Bhushan, Impact of nose radius and machining parameters on surface roughness, tool wear and tool life during turning of AA7075/SiC composites for green manufacturing, Mechanics of Advanced Materials and Modern Processes, 6(1) (2020) 1. https://doi.org/10.1186/s40759-020-00045-7.
[31] H. Saglam, S. Yaldiz, F. Unsacar, The effect of tool geometry and cutting speed on main cutting force and tool tip temperature, Materials & design, 28(1) (2007) 101-111. https://doi.org/10.1016/j.matdes.2005.05.015.
[32] H. Wang, J. Sun, J. Li, L. Lu, N. Li, Evaluation of cutting force and cutting temperature in milling carbon fiber-reinforced polymer composites, The International Journal of Advanced Manufacturing Technology, 82 (2016) 1517-1525. https://doi.org/10.1007/s00170-015-7479-2.
[33] M. Akgün, H. Yurtkuran, H. B. Ulas, AA7075 alaşımının işlenebilirliğine suni yaşlandırmanın etkisinin analizi ve kesme parametrelerinin optimizasyonu, Pamukkale Üniversitesi Mühendislik Bilimleri Dergisi, 26(1) (2020) 75-81. https://doi.org/10.5505/pajes.2019.71224.
[34] M. Akgün, H. Demir, and İ. Çiftçi, Optimization of surface roughness in turning Mg2Si particle reinforced magnesium, Politeknik Dergisi, 21(3) (2018) 645-650. https://doi.org/10.2339/politeknik.385481.
[35] U. Persson, H. Chandrasekaran. Machinability of martensitic steels in milling and the role of hardness. in Proc. 6th Int. Tooling Conf., Karlstad University, Sweden, 2002: 1225-1236.
[36] Ş. Bayraktar, G. Uzun, Experimental study on machinability of pre-hardened Toolox 44 and Nimax mould steels, J. Fac. Eng. Archit. Gazi Univ, 36 (2021) 1939-1947.
[37] S. K. Thangarasu, S. Shankar, A. Tony Thomas, G. Sridhar, Prediction of cutting force in turning process-an experimental approach, IOP conference series: materials science and engineering, 310 (2018) 012119. https://doi.org/10.1088/1757-899X/310/1/012119.
[38] M. K. Gupta, M. E. Korkmaz, M. Sarıkaya, G. M. Krolczyk, M. Günay, S. Wojciechowski, Cutting forces and temperature measurements in cryogenic assisted turning of AA2024-T351 alloy: An experimentally validated simulation approach, Measurement, 188 (2022) 110594. https://doi.org/10.1016/j.measurement.2021.110594.
[39] M. Kuntoğlu, O. Acar, M. K. Gupta, H. Sağlam, M. Sarikaya, K. Giasin, D. Y. Pimenov, Parametric optimization for cutting forces and material removal rate in the turning of AISI 5140. Machines, 9(5) (2021) 90. https://doi.org/10.3390/machines9050090.
[40] E. Salur, A. Aslan, M. Kuntoğlu, A. Güneş, Ö. S. Şahin, Optimization of cutting forces during turning of composite materials, Acad. Platf. J. Eng. Sci, 8 (2020) 423-431.
[41] T. Szecsi, Cutting force modeling using artificial neural networks, Journal of Materials Processing Technology, 92 (1999) 344-349. https://doi.org/10.1016/S0924-0136(99)00183-1.
[42] K. J. S. Kumar, R. N. Marigoudar, Comparative study of cutting force development during the machining of un-hybridized and hybridized ZA43 based metal matrix composites, Journal of the Mechanical Behavior of Materials, 28(1) (2019) 146-152. https://doi.org/10.1515/jmbm-2019-0016.
[43] A. Mahamani, Machinability study of Al-5Cu-TiB 2 in-situ metal matrix composites fabricated by flux-assisted synthesis, Journal of Minerals and Materials Characterization and Engineering, 10(13) (2011) 1243-1254.
[44] M. Aydın, Ti6Al4V Alaşımının ortogonal tornalanmasında ilerleme hızının kesme kuvveti ve talaş morfolojisi üzerindeki etkilerinin sonlu elemanlar analizi, Gazi Üniversitesi Fen Bilimleri Dergisi Part C: Tasarım ve Teknoloji, 12(2) (2024) 567-576. https://doi.org/10.29109/gujsc.1420233.
[45] C. Yao, Z. Zhou, J. Zhang, D. Wu, L. Tan, Experimental study on cutting force of face-turning Inconel718 with ceramic tools and carbide tools, Advances in Mechanical Engineering, 9(7) (2017) 9. https://doi.org/10.1177/1687814017716620.

[46] J. G. Lima, R. F. Avila, A. M. Abrao, M. Faustino, J. P. Davim, Hard turning: AISI 4340 high strength low alloy steel and AISI D2 cold work tool steel, Journal of Materials Processing Technology, 169(3) (2005) 388-395. https://doi.org/10.1016/j.jmatprotec.2005.04.082.
[47] H. Bouchelaghem, M. A. Yallese, T. Mabrouki, A. Amirat, J. F. Rigal, Experimental investigation and performance analyses of CBN insert in hard turning of cold work tool steel (D3), Machining Science and Technology, 14(4) (2010) 471-501. https://doi.org/10.1080/10910344.2010.533621.
[48] K. Kamdani, I. Ashaary, S. Hassan, M. A. Lajis, The effect of cutting force and tool wear in milling INCONEL 718. in Journal of Physics: Conference Series, (2019) 1-6.
[49] E. A. Rahim, H. Sasahara, Surface integrity when drilling nickel-based superalloy under MQL suppl, Key Engineering Materials, 443 (2010) 365-370. https://doi.org/10.4028/www.scientific.net/KEM.443.365.
[50] A. Taşlıyan, M. Acarer, U. Şeker, H. Gökkaya, B. Demir, Inconel 718 Süper Alaşiminin İşlenmesinde Kesme Parameterelerinin Kesme Kuvveti Üzerindeki Etkisi, Gazi Üniversitesi Mühendislik Mimarlık Fakültesi Dergisi, 22(1) (2007) 1-5.
[51] A. Ebrahimi, M. M. Moshksar, Evaluation of machinability in turning of microalloyed and quenched-tempered steels: Tool wear, statistical analysis, chip morphology, Journal of materials processing technology, 209(2) (2009) 910-921. https://doi.org/10.1016/j.jmatprotec.2008.02.067.
[52] K. Shi, D. Zhang, J. Ren, C. Yao, X. Huang, Effect of cutting parameters on machinability characteristics in milling of magnesium alloy with carbide tool, Advances in Mechanical Engineering, 8(1) (2016). https://doi.org/10.1177/1687814016628392.
[53] C. Kalyan, G. L. Samuel, Cutting mode analysis in high speed finish turning of AlMgSi alloy using edge chamfered PCD tools, Journal of Materials Processing Technology, 216 (2015) 146-159. https://doi.org/10.1016/j.jmatprotec.2014.09.003.
[54] A. Ercetin, K. Aslantaş, Ö. Özgün, M. Perçin, M. P. G. Chandrashekarappa, Optimization of machining parameters to minimize cutting forces and surface roughness in micro-milling of Mg13Sn alloy, Micromachines, 14(8) (2023) 1590. https://doi.org/10.3390/mi14081590.
[55] A. H. Tazehkandi, F. Pilehvarian, B. Davoodi, Experimental investigation on removing cutting fluid from turning of Inconel 725 with coated carbide tools, Journal of Cleaner Production, 80 (2014) 271-281. https://doi.org/10.1016/j.jclepro.2014.05.098.
[56] A. H. Tazehkandi, M. Shabgard, G. Kiani, F. Pilehvarian, Investigation of the influences of polycrystalline cubic boron nitride (PCBN) tool on the reduction of cutting fluid consumption and increase of machining parameters range in turning Inconel 783 using spray mode of cutting fluid with compressed air, Journal of Cleaner Production, 135 (2016)1637-1649. https://doi.org/10.1016/j.jclepro.2015.12.102.
[57] B. Özlü, Investigation of the effect of cutting parameters on cutting force, surface roughness and chip shape in turning of Sleipner cold work tool steel, Journal of the Faculty of Engineering and Architecture of Gazi University, 36(3) (2021) 1241-1251. https://doi.org/10.17341/gazimmfd.668169.
[58] I. Ciftci, Machining of austenitic stainless steels using CVD multi-layer coated cemented carbide tools, Tribology international, 39(6) (2006) 565-569. https://doi.org/10.1016/j.triboint.2005.05.005.
[59] K. Kadirgama, K. A. Abou-El-Hossein, M. M. Noor, K. V. Sharma, B. Mohammad, Tool life and wear mechanism when machining Hastelloy C-22HS, Wear, 270(3-4) (2011) 258-268. https://doi.org/10.1016/j.wear.2010.10.067.
[60] M. Sima, T. Özel, Modified material constitutive models for serrated chip formation simulations and experimental validation in machining of titanium alloy Ti–6Al–4V, International Journal of Machine Tools and Manufacture, 50(11) (2010) 943-960. https://doi.org/10.1016/j.ijmachtools.2010.08.004.
[61] S. E. Bernard, R. Selvaganesh, G. Khoshick, D. S. Raj, A novel contact area based analysis to study the thermo-mechanical effect of cutting edge radius using numerical and multi-sensor experimental investigation in turning, Journal of Materials Processing Technology, 293 (2021) 117085. https://doi.org/10.1016/j.jmatprotec.2021.117085.
[62] M. Wagih, M. A. Hassan, H. El-Hofy, J. Yan, I. Maher, Effects of process parameters on cutting forces, material removal rate, and specific energy in trochoidal milling, Proceedings of the Institution of Mechanical Engineers, Part C: Journal of Mechanical Engineering Science, 238(7) (2024) 2745-2757. https://doi.org/10.1177/09544062231196991.
[63] A. V. Muthusamy Subramanian, M. D. G. Nachimuthu, V. Cinnasamy, Assessment of cutting force and surface roughness in LM6/SiCp using response surface methodology, Journal of applied research and technology, 15(3) (2017) 283-296. https://doi.org/10.1016/j.jart.2017.01.013.
[64] S. Vijarangan, D. A. Budan, S. Arunachalam, T. Page, Effect of Fibre Position And Proportion On The Machinability Of GFRP Composites-An FEA And Merchant's Model, i-Manager's Journal on Future Engineering and Technology, 5(1) (2009) 33-43.
[65] Z. I. Korka, C. O. Micloşină, V. Cojocaru, An experimental study of the cutting forces in metal turning, Analele Universităłi "Eftımie Murgu" Reşiła Anul XX, (2) (2013) 25-32.
[66] P. Moradpour, F. Scholz, K. Doosthoseini, A. Tarmian, Measurement of wood cutting forces during bandsawing using piezoelectric dynamometer. Drv. Ind, 67 **(**2016) 79-84.
[67] H. Gökkaya, AA5052 Alaşiminin işlenmesinde işleme parametrelerinin kesme kuvveti ve yüzey pürüzlülüğüne etkisinin deneysel olarak incelenmesi, Pamukkale Üniversitesi Mühendislik Bilimleri Dergisi, 12(3) (2011) 295-301.

[68] A. S. Shouckry, The effect of cutting conditions on dimensional accuracy, Wear, 80(2) (1982) 197-205. https://doi.org/10.1016/0043-1648(82)90217-4.
[69] E. Usui, T. Shirakashi, T. Kitagawa, Analytical prediction of cutting tool wear, Wear, 100(1-3) (1984) 129-151. https://doi.org/10.1016/0043-1648(84)90010-3.
[70] G. Byrne, Thermoelectric signal characteristics and average interfacial temperatures in the machining of metals under geometrically defined conditions, International Journal of Machine Tools and Manufacture, 27(2) 1987 215-224. https://doi.org/10.1016/S0890-6955(87)80051-2.
[71] P. D. Muraka, G. Barrow, S. Hinduja, Influence of the process variables on the temperature distribution in orthogonal machining using the finite element method, International Journal of Mechanical Sciences, 21(8) (1979) 445-456. https://doi.org/10.1016/0020-7403(79)90007-9.
[72] A. Uysal, Effects of cutting parameters on drilling performance of carbon black–reinforced polymer composite, Proceedings of the Institution of Mechanical Engineers, Part B: Journal of Engineering Manufacture, 232(7) (2018) 1133-1142. https://doi.org/10.1177/0954405416662084.
[73] U. Çaydaş, M. Çelik, AA 7075-T6 alaşımının delinmesinde kesme parametrelerinin yüzey pürüzlülüğü, takım sıcaklığı ve ilerleme kuvvetine etkilerinin araştırılması, Politeknik Dergisi, 20(2) (2017) 419-425.
[74] A. Hosokawa, K. Kosugi, T. Ueda, Turning characteristics of titanium alloy Ti-6Al-4V with high-pressure cutting fluid, CIRP Annals, 71(1) (2022) 81-84. https://doi.org/10.1016/j.cirp.2022.04.064.
[75] R. Kumar, A. K. Sahoo, K. Satyanarayana, G. Rao, Some studies on cutting force and temperature in machining Ti-6Al-4V alloy using regression analysis and ANOVA, Int J Ind Eng Comput, 4(3) (2013) 427-436. https://doi.org/10.5267/j.ijiec.2013.03.002.
[76] H. M. Mohammad, R. H. Ibrahim, Effect Of Cutting Parameters On Surface Roughness And Cutting Tool Temperature In Turning AISI 1045 Steel, University of Thi-Qar Journal for Engineering Sciences, 8(2) (2017) 127-137.
[77] J. Rodríguez, P. Muñoz-Escalona, Z. Cassier, Influence of cutting parameters and material properties on cutting temperature when turning stainless steel, Revista de la Facultad de Ingeniería Universidad Central de Venezuela, 26(1) (2011) 71-80.
[78] I. Espinoza-Torres, I. Martínez-Ramírez, J. M. Sierra-Hernández, D. Jauregui-Vazquez, M. E. Gutiérrez-Rivera, F. D. J. T. D. Carmen, T. Lozano-Hernández, Measurement of Cutting Temperature in Interrupted Machining Using Optical Spectrometry, Sensors, 23(21) (2023) 8968. https://doi.org/10.3390/s23218968.
[79] E. Abdelnasser, A. Barakat, S. Elsanabary, A. Nassef, A. Elkaseer, Precision hard turning of Ti6Al4V using polycrystalline diamond inserts: surface quality, cutting temperature and productivity in conventional and high-speed machining, Materials, 13(24) (2020) 5677. https://doi.org/10.3390/ma13245677.
[80] M. Soori, B. Arezoo, Effect of cutting parameters on tool life and cutting temperature in milling of AISI 1038 carbon steel, Journal of New Technology and Materials, 13 (2023) 33-48. https://hal.science/hal-04111841v1.
[81] H. B. He, H. Y. Li, J. Yang, X. Y. Zhang, Q. B. Yue, X. Jiang, S. Lyu, A study on major factors influencing dry cutting temperature of AISI 304 stainless steel, International Journal of Precision Engineering and Manufacturing, 18 (2017) 1387-1392. https://doi.org/10.1007/s12541-017-0165-6.
[82] S. M. Lubis, S. Darmawan'Adianto. Effect of cutting speed on temperature cutting tools and surface roughness of AISI 4340 steel, in IOP Conference Series: Materials Science and Engineering, (2019) 012053. https://doi.org/10.1088/1757-899X/508/1/012053.
[83] D. Liu, Y. Zhang, M. Luo, D. Zhang, Investigation of tool wear and chip morphology in dry trochoidal milling of titanium alloy Ti–6Al–4V, Materials, 12(12) (2019) 1937. https://doi.org/10.3390/ma12121937.
[84] K. Yang, Y. Liang, K. Zheng, Q. Bai, W. Chen, *T*ool edge radius effect on cutting temperature in micro-end-milling process, The International Journal of Advanced Manufacturing Technology, 52 (2011) 905-912. https://doi.org/10.1007/s00170-010-2795-z.
[85] B. Akın, AISI 316L paslanmaz çeliklerin tornalanmasında yüzey pürüzlülüğünün incelenmesi, Yüksek Lisans Tezi, Selçuk Üniversitesi, Fen Bilimleri Enstitüsü, 2014.
[86] D. Bajić, B. Lela, D. Živković, Modeling of machined surface roughness and optimization of cutting parameters in face milling, Metalurgija, 47(4) (2008) 331-334.
[87] Ü. Karagöz, CNC ile işlemede ahşap malzemenin yüzey kalitesini etkileyen faktörler, Kastamonu University Journal of Forestry Faculty, 11(1) (2011) 18-26.
[88] M. Özdemir, Yüzey pürüzlülüğü üzerinde kesme parametrelerinin etki oranlarının Yüzey Yanıt Yöntemi kullanarak Analizi, Gazi University Journal of Science Part C: Design and Technology, 7(3) (2019) 639-648. http://dergipark.gov.tr/gujsc.
[89] B. Karayel, M. Nalbant, Ç4140 Malzemesinin Tornalamasinda İlerleme, Kesme Hizi Ve Kesici Takimin Yüzey Pürüzlülüğü, Takim Ömrü Ve Aşinmaya Etkileri, Makine Teknolojileri Elektronik Dergisi, 11(3) (2014) 11-26.
[90] N. Kavak, AISI 1040 çeliğinin kuru tornalanmasında yüzey pürüzlülüğünün incelenmesi, Karaelmas Fen ve Mühendislik Dergisi, 2(2) (2012) 24-29.
[91] L. Uğur, 7075 Alüminyum Malzemesinin Frezelenmesinde Yüzey Pürüzlülüğünün Yanıt Yüzey Metodu İle Optimizasyonu, Erzincan University Journal of Science and Technology, 12(1) (2019) 326-335.
[92] H. Demirpolat, K. Kaya, R. Binali, M. Kuntoğlu, AISI 52100 Rulman Çeliğinin Tornalanmasında İşleme Parametrelerinin Yüzey Pürüzlülüğü, Kesme Sıcaklığı ve Kesme Kuvveti Üzerindeki Etkilerinin İncelenmesi, İmalat Teknolojileri ve Uygulamaları, 4(3) (2023) 179-189. https://doi.org/10.52795/mateca.1393430.

[93] M. Nalbant, H. Gökkaya, G. Sur, Application of Taguchi method in the optimization of cutting parameters for surface roughness in turning, Materials & design, 28(4) (2007) 1379-1385. https://doi.org/10.1016/j.matdes.2006.01.008.
[94] X. Wang, C. X. Feng, Development of empirical models for surface roughness prediction in finish turning, The International Journal of Advanced Manufacturing Technology, 20 (2002) 348-356. https://doi.org/10.1007/s001700200162.
[95] A. Hasçelik, K. Aslantaş, Mikro Tornalama İşleminde Kesici Takım Burun Yarıçapının Kesme Kuvvetlerine Etkisi, Journal of Materials and Mechatronics: A, 2(1) (2021) 13-25.
[96] R. Binali, H. Demirpolat, M. Kuntoğlu, K. Kaya, Exploring the Tribological Performance of Mist Lubrication Technique on Machinability Characteristics During Turning S235JR Steel, Manufacturing Technologies and Applications, 5(3) (2024) 276-283. https://doi.org/10.52795/mateca.1541090.
[97] X. Chuangwen, D. Jianming, C. Yuzhen, L. Huaiyuan, S. Zhicheng, X. Jing, The relationships between cutting parameters, tool wear, cutting force and vibration, Advances in Mechanical Engineering, 10(1) (2018). https://doi.org/10.1177/1687814017750434.
[98] M. Özdemir, K. Ercan, B. Büyüker, H. K. Akyıldız, Analysis of the effect of tool nose radius, feed rate, and cutting depth parameters on surface roughness and cutting force in CNC lathe machining of 36CrNiMo4 alloy steel, Gazi University Journal of Science Part A: Engineering and Innovation, 8(2) (2021) 308-317.
[99] M. Kuruc, T. Vopát, J. Peterka, M. Necpal, V. Šimna, J. Milde, F. Jurina, The influence of cutting parameters on plastic deformation and chip compression during the turning of C45 medium carbon steel and 62SiMnCr4 tool steel, Materials, 15(2) (2022) 585. https://doi.org/10.3390/ma15020585.
[100] J. O'Hara, F. Fang, Advances in micro cutting tool design and fabrication, International journal of Extreme Manufacturing, 1(3) (2019) 032003. https://doi.org/10.1088/2631-7990/ab3e7f.